N85-25883

LEARJET MODEL 55 WING ANALYSIS WITH LANDING LOADS

Robert R. Boroughs
Gates Learjet Corporation

SUMMARY

NASTRAN analysis has been used to determine the impact of new landing loads on the Learjet Model 55 wing. These new landing loads were the result of a performance improvement effort to increase the landing weight of the aircraft to 18,000 lbs. from 17,000 lbs. and extend the life of the tires and brakes by incorporating larger tires and heavy duty brakes. Landing loads for the original 17,000 lb. airplane landing configuration were applied to the full airplane NASTRAN model. These analytical results were correlated with the strain gage data from the original landing load static tests. Then, the landing loads for the 18,000 lb. airplane were applied to the full airplane NASTRAN model, and a comparison was made with the original Model 55 data. The results of this comparison enabled Learjet to determine the difference in stress distribution in the wing due to these two different sets of landing loads, and consequently, this comparison helped Learjet to reduce the number of tests that would have otherwise been necessary.

INTRODUCTION

The Learjet Model 55 wing has evolved from the Learjet 28/29 wing (see ref. 1). Both the Model 55 and 28/29 wings are similar to the Learjet 35/36 wing geometrically (see ref. 2) except that the two foot wing extension and tip tank on the Model 35/36 wing is replaced by a six foot extension and a wingle on the Model 28/29 and Model 55 wing. The Model 55 wing is fabricated using eight spars and eight ribs per side. This network of spars and ribs is covered with a machined aluminum skin on both the top and bottom surfaces. However, the skin thicknesses and spar section properties are very different from the previous Model 35/36 wing (see ref. 1).

Attachment of the wing to the fuselage is accomplished through eight fittings. The fitting locations are distributed equally between the right and left with four attachment points on each side of the fuselage. These four points in the wing are located at spars two, five, seven and eight. A centerline splice plate provides the carry-through capability to connect the right hand and the left hand halves of the wing, thus allowing the wing to be continuous through the fuselage.

The main landing gear is supported in the wing at the forward end of the trunnion arm by a fitting integral with spar five and at the aft end of the trunnion arm by a fitting integral with spar seven. These two support fittings also serve as the pivot points for landing gear extension and retraction. Actuation of the main landing gear is achieved by a hydraulic cylinder which attaches to the landing gear cylinder at the outboard end and at spar seven on the inboard end. The main landing gear is a dual wheel air-oil type gear with an aluminum cylinder and a steel piston.

BACKGROUND

The Learjet Model 55 aircraft was originally certified by the Federal Aviation Administration in March of 1981. In 1984 a performance improvement package was made available for the Model 55 aircraft as an option to the basic configuration. This option permitted an increase in takeoff and landing weight with the incorporation of a larger set of tires and brakes on the main landing gear. The takeoff weight was increased to 21,500 lbs. from 21,000 lbs., and the landing weight was increased to 18,000 lbs. from 17,000 lbs.

This increase in takeoff and landing weight necessitated the development of a new set of loads for these conditions. The results of these new load calculations revealed that the increase in landing weight had more of an impact on the wing structure than the increase in takeoff weight. Consequently, most of the analytical effort was directed toward resolving the differences between the original Model 55 landing loads and the new landing loads. The original landing loads for the Model 55 were developed using conventional static aeroelastic methods, but since the time when these data were generated, Learjet has developed the analytical capability to generate flexible body dynamic landing loads. These flexible body dynamic loads have been demonstrated to be more realistic than the more conservative static aeroelastic landing loads for many applications. Dynamic flexible body loads are also almost always lower than the static aeroelastic landing loads. Consequently, there was good reason to believe that the landing loads developed with the flexible body dynamic methods for an 18,000 lb. airplane could be less than or equal to the landing loads developed with static aeroelastic methods for a 17,000 lb. airplane.

Since the landing loads on the wing consisted of one "G" airloads as well as main landing gear loads, a method was needed to verify that the net effect of the new 18,000 lb. aircraft landing loads on the wing was less severe than that of the older 17,000 lb. aircraft landing loads. NASTRAN analysis was proposed as a method to help determine the impact of the new 18,000 lb. landing weight loads on the Model 55 wing structure. A finite element model was available of the complete Learjet Model 55 aircraft, and these types of load conditions had been run earlier for the 17,000 lb. landing weight condition.

MODELING CRITERIA

The NASTRAN model for the Learjet 55 aircraft included the full fuselage, vertical tail and complete wing and consisted of over 16,000 elements and 26,000 degrees of freedom. The original model used substructuring techniques (see ref. 3) in the finite element analysis mainly due to the limitations and restrictions on computer resources that were available during that time period. However, since then, Learjet has acquired and installed an IBM 3033 and an IBM 3081. Both of these main frames are much faster and have more memory and disk space than was available on the previous in-house IBM 370-158. These new computers allowed Learjet to run the full aircraft model without using substructure techniques on a regular overnight turnaround basis.

Geometry in the finite element model is defined extensively through the use of local coordinate systems. Almost all installations in the aircraft model are defined in a local coordinate system which is more oriented to the geometry of that installation as opposed to the basic coordinate system definition. Another reason for using local coordinate systems is to provide flexibility for future modifications

and additions such as a fuselage plug. These changes could then easily be accommodated by simply changing the origin of the appropriate local coordinate systems. Sufficient intervals in node and element numbering were also established to facilitate this type of model revision. A total of 102 local coordinate systems are used in the model with this number being almost equally divided between rectangular and cylindrical coordinate system.

The wing and main landing gear are modeled using five local rectangular coordinate systems. The right hand half of the wing is modeled in one local rectangular system and the left hand half of the wing is modeled in a second local rectangular system. A third rectangular system is used to model the wing centerline rib which is in a plane parallel to the centerline plane of the airplane. Each main landing gear is defined in a local rectangular system with the positive "Z" axis directed aft from the forward pivot point to the aft pivot point and with the positive "X" axis pointing down (see fig. 1). Since the landing gear elements are to simulate the static test conditions with the main concern being the wing and wing support structure, the hydraulic characteristics of the gear are not included in the NASTRAN model. The landing gear was modeled with the intent of representing the geometry and stiffness of the gear so that the landing loads would be transferred accurately into the wing structure.

Attachment of the wing to the fuselage is accomplished through four fittings on each side of the fuselage. These eight fittings are represented in the model with the appropriate stiffness and degrees of freedom to reflect the load paths from the wing to the fuselage. The wing is bolted to the fuselage at these fitting points with a single bolt, and each joint is modeled to simulate a pinned connection. However, the fitting at spar five in the wing in addition to being pinned also transfers drag load, and this degree of freedom had to be included at that joint.

FUSELAGE

A complete representation of the fuselage structure is included in the NASTRAN analysis basically because the model was already in this format, and this version could easily be run overnight. Another reason for using this configuration was that an accurate definition was desired of the wing to fuselage internal loads and the wing internal loads and stresses in the members adjacent to the attachment points. The fuselage geometry is generally defined with grid points on the outside contour being located at frame and stringer intersections. Almost all of these grid points were defined in local cylindrical coordinate systems which were established at each frame location. Interior grid points such as those on bulkheads were usually located at the intersections of beams and intercostals. These interior grid points were defined in local rectangular coordinate systems which were also created at each frame location (see ref. 3).

The outer surface of the fuselage, or skin covering, is modeled using the QDMEM2 membrane element (see ref. 4). Simulation of the frame members bending capability is accomplished using BAR elements. Stringers are represented using the axial load capability in the CONROD element, and intercostals and beams are modeled using BAR elements. QUAD1 elements are used to simulate the aluminum honeycomb aft pressure bulkhead and the baggage floor over the wing. A significant feature simulated in the fuselage model is the cabin door and the escape/baggage door. These members are modeled with a double row of nodes along the door boundary. One row of nodes defines the cutout in the fuselage, and the second row of nodes defines the

edge of the door. The cabin door is split at the mid-line into an upper and lower door with the upper half being hinged on the upper edge and the lower half being hinged at the lower edge. In the closed position the door is secured by shear pins and tension lugs along the forward and aft edges. The escape/baggage door is of similar type construction except that this member is a one-piece type construction and is hinged only on the upper edge, and tension lugs are not used.

Another major feature simulated in the fuselage section with considerable detail is the cutout to allow the wing to pass through the fuselage. The lower portion of the fuselage at the wing intersection is essentially designed around the wing. Structure in this region had to have the capability of transferring fuselage bending and pressure loads around the wing. The forward portion of the cutout is sealed by a partial bulkhead at frame 24, while the aft portion of the cutout is sealed by another partial bulkhead at frame 31. An aluminum honeycomb floor panel is installed just above the wing to seal the upper portion of this cutout in the cabin pressure vessel. Once the wing is attached to the fuselage, a removable keel beam is installed across the lower portion of this cutout connecting frame 24 and frame 31. The keel beam basically extends from the forward pressure bulkhead almost all the way to the vertical tail attachment structure in one form or another. In the forward fuselage this structure is of dual "I" beam construction and extends from the forward pressure bulkhead to the forward edge of the wing cutout in the fuselage at frame 24. Beneath the wing the keel beam is fabricated as a closed box section (see fig. 2 & 3). This type of construction is also used aft of the wing cutout in the fuselage, although in this portion of the fuselage the keel beam is integrated with the frame and stringer construction.

Elements used to represent the structure in the partial bulkhead at frame 24 are BAR members for the beams and stiffners and QDMEM2 membranes for the webs. Modeling of the partial bulkhead at frame 31 is accomplished using BAR elements for the beams and stiffners and QUAD2 plates for the bulkhead webs. The keel beam is basically modeled using CONRODS for the caps and SHEAR elements for the vertical webs. Beneath the wing, where the keel beam is a closed box section, QDMEM2 panels are used to simulate the skin covers. Additional details on the fuselage model can be found in ref. 3.

WING

The entire wing is simulated in the finite element model by duplicating the right hand half from the left hand half. Each half of the wing is modeled in a separate local rectangular coordinate system. The local coordinate system for the left wing had the X axis positive aft, the Y axis positive left hand outboard, and the Z axis positive down. The local rectangular system for the right hand wing is oriented with the X axis positive forward, the Y axis positive right hand outboard, and the Z axis positive down. Since the centerline rib is not really oriented in either one of these coordinate systems, this member is modeled in a third local rectangular coordinate system. This local system is established with the X axis positive aft, the Y axis positive left hand outboard, and the Z axis positive down.

Grid points for the wing are located at the outer contour along the spar mold lines. Since the Learjet 55 wing is basically an eight spar wing in the inboard section and a ten spar wing in the outboard section no more grid points were added in between the spars. The spacing between ribs is much greater than the spacing between the spars, and consequently the distance between ribs is divided into four

or five bays in order to obtain square panels as best as possible.

The Learjet 55 wing is an all aluminum type fabrication. Spar members are basically designed to be continuous while most of the ribs are designed as segmented elements with the exception of the centerline rib and the landing gear rib at the outboard end of the wheel well. Wing skins are generally fabricated in two pieces with a wing skin splice in the outboard section at W.S. 181. Centerline skin splices on the top and bottom are used to join the right hand and left hand halves of the wing. ROD elements are used to model the spar caps and rib caps while SHEAR elements are used to represent the spar and rib webs. The skin and skin splices are simulated using QDMEM2 membrane elements. Fittings and other attachment members are generally modeled using BAR elements. Additional details on the wing model can be found in ref. 1.

WING TO FUSELAGE ATTACHMENT

Attachment of the wing to the fuselage is accomplished with four fittings on each side of the fuselage. These fittings are symmetrically located from the right hand side to the left hand side and are positioned in the wing at the intersection of the fuselage attachment rib at spars two, five, seven and eight. All ribs in the wing are located on constant wing station lines except the fuselage attachment rib which follows the outer contour of the fuselage. The attachment at spar two is a linkage type joint with a strap pinned at both the fuselage and wing ends. The fitting at spar five has the capability to transfer vertical, side, and drag loads, while the fittings at spars seven and eight can only transfer vertical and side loads (single pinned joint).

Four frame locations were created in the fuselage to match the four fitting points on the wing. These support points are frame 25 which matches the wing fitting at spar two, frame 27 which corresponds to the spar five wing fitting, frame 29 which is located over the spar seven wing fitting, and frame 30 which is positioned above the wing fitting at spar eight. These frames are actually double frames with a plate connecting the inner flanges to form a closed box cross section. This reinforcement is necessary to provide sufficient stiffness and an adequate load path and redistribution system for transferring wing reactions into the fuselage.

Each of the double frames over the wing attach fittings are modeled using BAR elements. The use of BAR elements helps to reduce the number of degrees of freedom that would have otherwise been required to simulate this structure. BAR elements are also used to represent the fuselage attach fittings at the bottom of the double frames at all four locations on each side of the airplane. The lower end of these fittings is pin flagged in the third rotational degree of freedom, and the fittings at frames 29 and 30 are also pin flagged in the fore and aft translational degree of freedom.

Attachment fittings on the wing are generally separated into that portion of the fitting that is internal to the wing and that portion which extends outside the wing contour. The portion of the wing fitting that is inside the wing contour is generally designed to reinforce the local internal structure to carry large concentrated loads. These loads are transferred to the fitting from the adjacent spars, ribs, and wing skin. BAR elements are used to simulate these internal fitting members in the NASTRAN finite element model. The portion of the wing fitting which extends above the wing contour is also modeled using BAR elements. These members

provide load transfer capability in all six degrees of freedom at the lower end, but at the upper end of the BAR element the rotation about the fore and aft axis is pin flagged at all four fittings per side, and the drag translational degree of freedom is pin flagged at spars one, seven, and eight. The drag load capability is not released at spar five since this fitting is designed as the main drag load reaction path. Arrangement of these fittings in the finite element model can be seen in figures 3 and 4.

LANDING GEAR

Each main landing gear is modeled in a separate local rectangular coordinate system. These local rectangular systems are defined with respect to the wing local rectangular system with the landing gear local Z axis oriented along the gear retraction pivot axis and pointing aft. The landing gear cylinder is defined in the X-Z plane so that when the main landing gear is extended the X axis positive direction is pointing down toward the wheels. Consequently, the positive Y axis is always oriented toward the right for both the left hand and right hand gears in the down position.

Since the main landing gear simulation was to be a part of a much larger finite element model, a simplified representation of the gear was established for this project. The geometry of the gear is defined with the piston in the 25 percent compressed position. This geometry was incorporated to facilitate the application of the critical landing loads which were defined with the landing gear in this position. This position of the gear was used on the previous Model 55 static tests, and the main concern in this analysis was to be able to correlate the NASTRAN results with the strain gage data on the wing rather than simulating the functional characteristics of the main landing gear. The effect of the piston sliding inside the cylinder and the compressibility of the air-oil mixture in the piston and the cylinder are not simulated in this model. Using these guidelines, grid points are located along the center of the cylinder, piston, and axle to represent not only the center line geometry, but also the major points where section property changes occur in these members. BAR elements are used to model all parts of the cylinder, piston and axle.

Extension and retraction of the gear is achieved by means of a hydraulic actuator which attaches to a lug on the landing gear cylinder on the outboard end and to a fitting on spar seven on the inboard end (see fig. 5). This actuator is basically pinned at each end, and when the gear is extended the actuator has a locking mechanism which locks the gear into the down position. Since this system is pinned at each end, a ROD element is used to represent the actuator system stiffness (see fig. 6).

Attachment of the main landing gear to the wing is achieved at three support points (see fig. 5). Two of these points are at the upper end of the landing gear assembly. The first point, or forward support, is located at spar five, while the second point, or aft support, is located at spar seven. A group of four BAR elements is used to simulate each of the trunnion fittings. All four BAR elements are connected at one end to the grid point which defines the intersection of the trunnion pivot axis and the mid-plane of the support fitting lug. Two of these BAR elements are connected to two separate points on the upper spar cap while the other two BAR elements are connected to two separate points on the lower spar cap. This connectivity arrangement is very similar for both the forward and aft trunnion support fittings. The third attachment point for the main landing gear is the actuator

support fitting located on spar seven at the inboard end of the wheel well. This fitting is also modeled with BAR elements using the same concept as the other two fittings (see fig. 6). The grid point which represents the inboard actuator support point is defined at the location where the actuator is pinned to the support fitting.

CONSTRAINTS

Since the loads to be applied to the aircraft model consist of landing gear and air loads on the wing and balancing loads on the fuselage, only a minimal number of constraints are required to maintain equilibrium. The constraints on the model are established mainly to neutralize any unbalanced rotations rather than serving as major reaction points. Consequently, constraints are established at two points on the forward pressure bulkhead and at two points on the top of the vertical tail. The two points on the forward pressure bulkhead are located on the maximum breadth line of that fuselage cross section at the outside contour on the left hand and right hand sides. These grid points are constrained in the three translational degrees of freedom. Constraints on the vertical tail are located at the two outboard points of the horizontal tail pivot fitting where the horizontal tail attaches to the vertical tail. The horizontal tail is not included in this analysis, since this structure is not necessary for this load case, and the removal of this assembly from the finite element model reduces the size of the problem. All three translational degrees of freedom are constrained at these grid points on the top of the vertical tail as was done on the two grid points on the forward pressure bulkhead.

LOADS

Landing loads applied to the wing consist of the main landing gear spin up and spring back conditions with one "G" wing air loads. Generally speaking, the main gear spin up condition is the most critical for this analysis. The loads applied to the main gear are distributed on a 60% and 40% basis between the outboard wheel and inboard wheel respectively. This distribution is applied to both the vertical and drag load components. Wheel loads are applied to the main gear axle at the centerline of the wheel with the vertical and drag components being normal and parallel to the ground, and in the NASTRAN mdoel these loads are defined in the basic coordinate system (fuselage reference system). The one "G" wing air loads are applied to simulate the air loads experienced by the wing at the moment of touchdown by the aircraft. These loads are distributed over the outboard portion of the wing and are located toward the aft chord of the wing, since this is a maximum nose down torque condition.

The loads for the increased landing weight cases were generated using a dynamic landing computer program which was not available during the original Model 55 certification effort. Original Model 55 landing loads were developed using a conventional static aeroelastic program. These loads are conservative, since the static aeroelastic theory did not account for the aircraft flexibility and response. Landing loads calculated using the new dynamic landing program normally gave lower loads for the same conditions as opposed to the static aeroelastic program. Consequently, there was good reason to expect that the impact of the new landing loads on the wing would be less than or equal to the old landing loads. The one "G" wing air loads are distributed so as to produce the correct shear moment and torque defined about the elastic axis of the wing. Both the landing gear loads and the one "G" wing air loads are applied to the NASTRAN model using FORCE cards. The balancing fuselage

loads are applied symmetrically between the right hand side and left hand side of the fuselage at the maximum breadth point of the frames and at the engine support points, and these loads are also defined using FORCE cards.

ANALYTICAL RESULTS

NASTRAN runs were made for the critical landing conditions. Since the wing skin stresses were below the buckling allowable, a wing skin buckling simulation was not performed on this project as has been done on previous maximum wing bending conditions. The first series of NASTRAN runs were made for the original Model 55 landing conditions with a 17,000 lb. landing weight. A correlation analysis was performed with these data and the strain gage data from the Model 55 landing condition static test. Plots were made of the upper and lower spar cap NASTRAN stresses and the strain gage data for spars five, seven and eight. Spar five was the gear forward support point and the forward boundary of the wheel well, and spar seven served as the gear aft support point and the aft boundary of the wheel well. These data have been plotted in figures 7 through 12. A comparison of the NASTRAN analytical results with the static test strain gage data shown in these figures indicated that the NASTRAN data agreed very well with the experimental data in almost all areas. Consequently, the NASTRAN analysis was considered a justifiable approach for comparing the original Model 55 landing conditions at the 17,000 lb. landing weight with the new Model 55 landing conditions using an 18,000 lb. landing weight.

The second series of NASTRAN runs were made with the new Model 55 landing conditions at the 18,000 lb. landing weight. Loads applied in these conditions were developed using the dynamic landing methods while the original Model 55 loads were generated using the static aeroelastic techniques. The results of these runs were also plotted along with the original Model 55 analytical results and test data and can be seen in figures 7 through 12. Stresses in the spar caps for the new landing conditions were generally less than the stresses in the spar caps for the original Model 55 landing conditions. In those areas where the stresses due to the new 18,000 lb. landing weight loads were not less than the stresses due to the old 17,000 lb. landing weight loads, the margins of safety were normally quite high. A comparison of the stresses resulting from these two load conditions can be seen in these six figures.

Since the highest stresses in almost all areas of the wing were lower for the new loading conditions, or the margins of safety were quite high in those areas where the stresses for the new load conditions were greater than the stresses due to the older load conditions, Learjet was able to reduce the number of static test conditions that were required for this program. The need for a full schedule of wing tests using the new landing load conditions was eliminated from the certification program as well as many of the individual landing gear static tests.

CONCLUDING REMARKS

A series of NASTRAN finite element analyses have been performed on the Learjet Model 55 aircraft to help determine the structural impact of increasing the aircraft landing weight to 18,000 lbs. from 17,000 lbs. The correlation of the NASTRAN analysis for the 17,000 lb. aircraft landing condition with the strain gage data from the corresponding static test demonstrated that the NASTRAN results simulated this condition very closely. Therefore, the NASTRAN model was considered to be an accurate

representation of the wing and wing support structure. A comparison of the NASTRAN results using the landing loads for an 18,000 lb. airplane with the NASTRAN results using the landing loads for a 17,000 lb. airplane revealed that the highest stresses in almost all areas of the wing were less due to the new load condition. In those areas of the wing where the stresses due to the new loads exceeded the stresses due to the original Model 55 loads, margin of safety calculations indicated that the structure was more than adequate. Consequently, the results of this NASTRAN analysis helped Learjet to significantly reduce the number of static test conditions that had to be conducted during the development of this performance improvement capability for the Learjet Model 55 aircraft.

REFERENCES

1. Boroughs, Robert R., "Development of the Learjet 28/29 Wing Using NASTRAN Analysis", pp 11-32, Eighth NASTRAN User's Colloquium, NASA CP 2131, October 1979.

2. Abla, Mike H., Boroughs, Robert R., and Cook, Everett L., "Analysis of the Learjet 35/36 Wing and Correlation With Experimental Results", NASTRAN User's Experiences, NASA TMX-3428, October 1976, pp 331-352.

3. Boroughs, Robert R., Paramasivam, Sivam, and Werner, Joanna K., "Development and Analysis of the Learjet 54/55 Fuselage NASTRAN Model Using Substructure Techniques", Ninth NASTRAN User's Colloquium, NASA CP 2151, October 1980.

4. The NASTRAN User's Manual, NASA SP-222(06), Washington, D.C., September 1983.

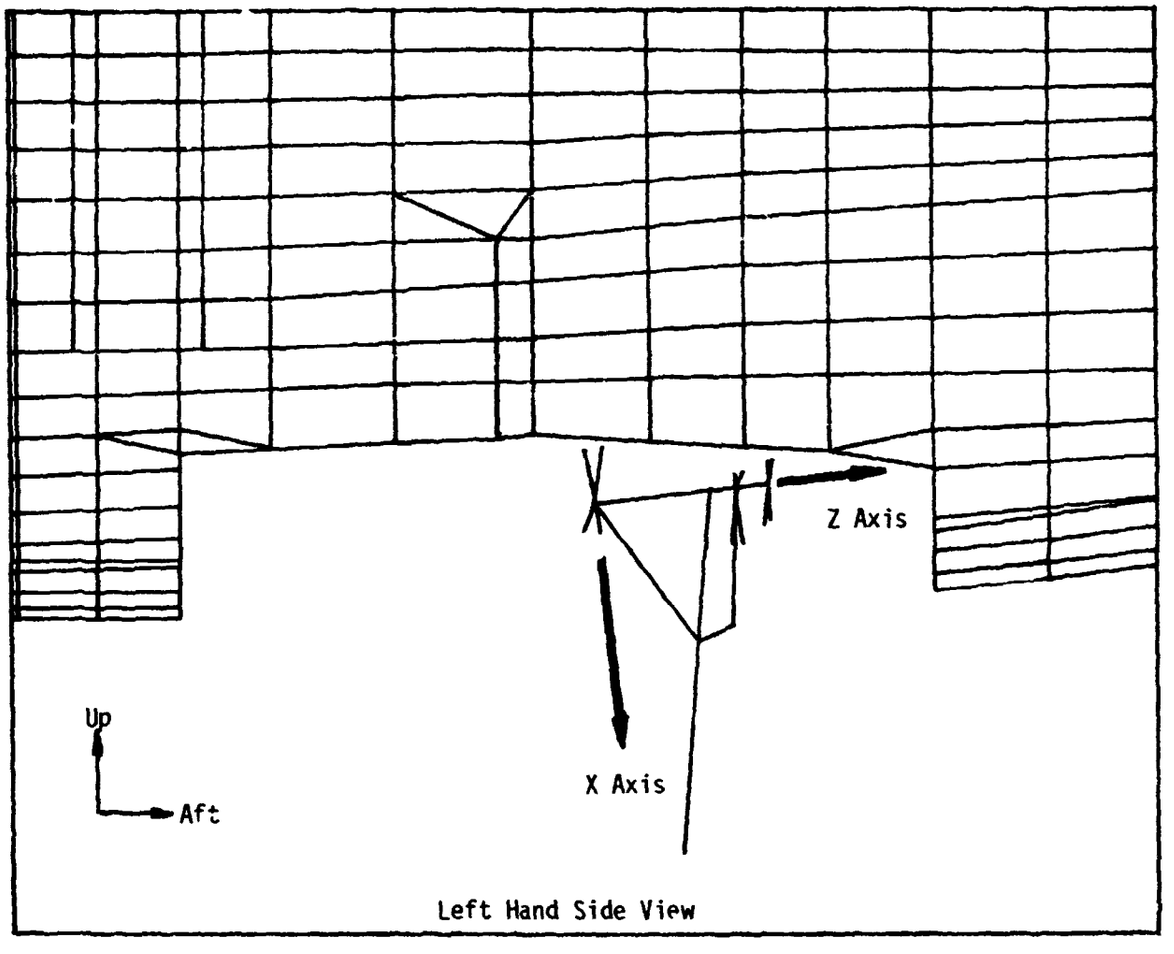

Figure 1 - Landing Gear Coordinate System

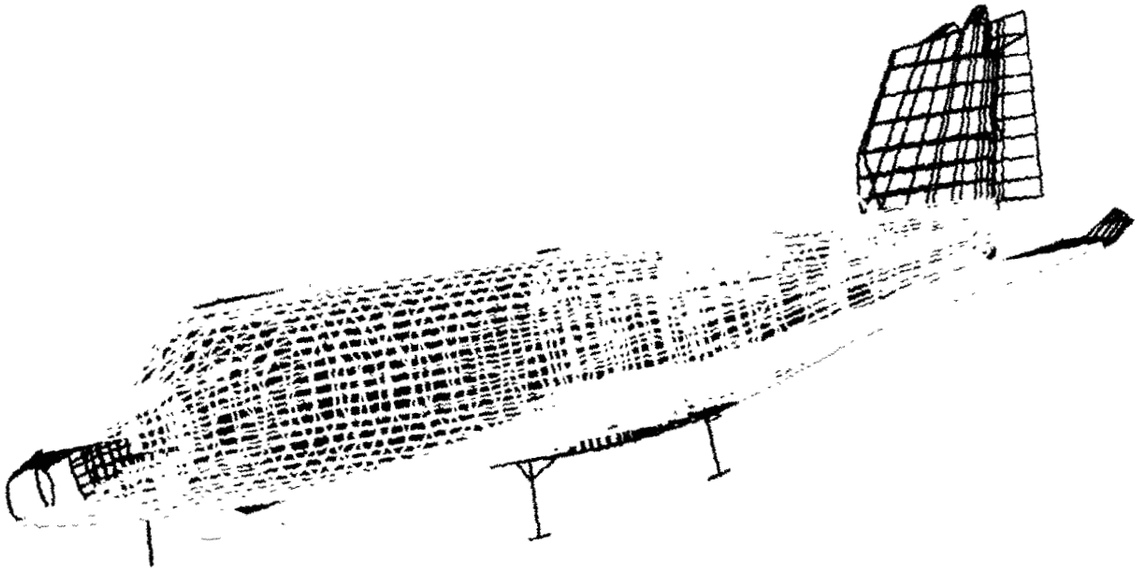

Figure 2 - Learjet 55 NASTRAN model

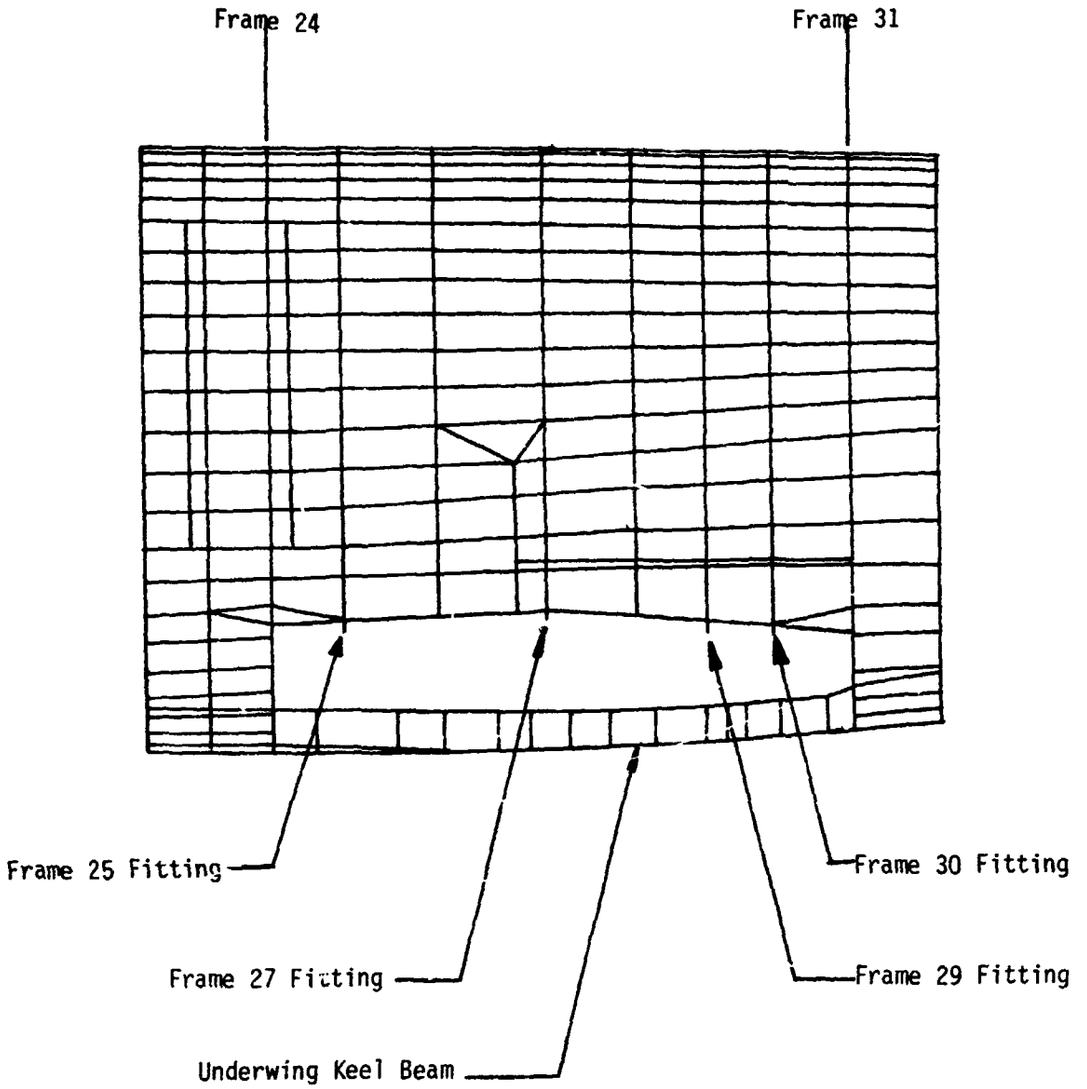

Figure 3 - Fuselage Attach Fittings

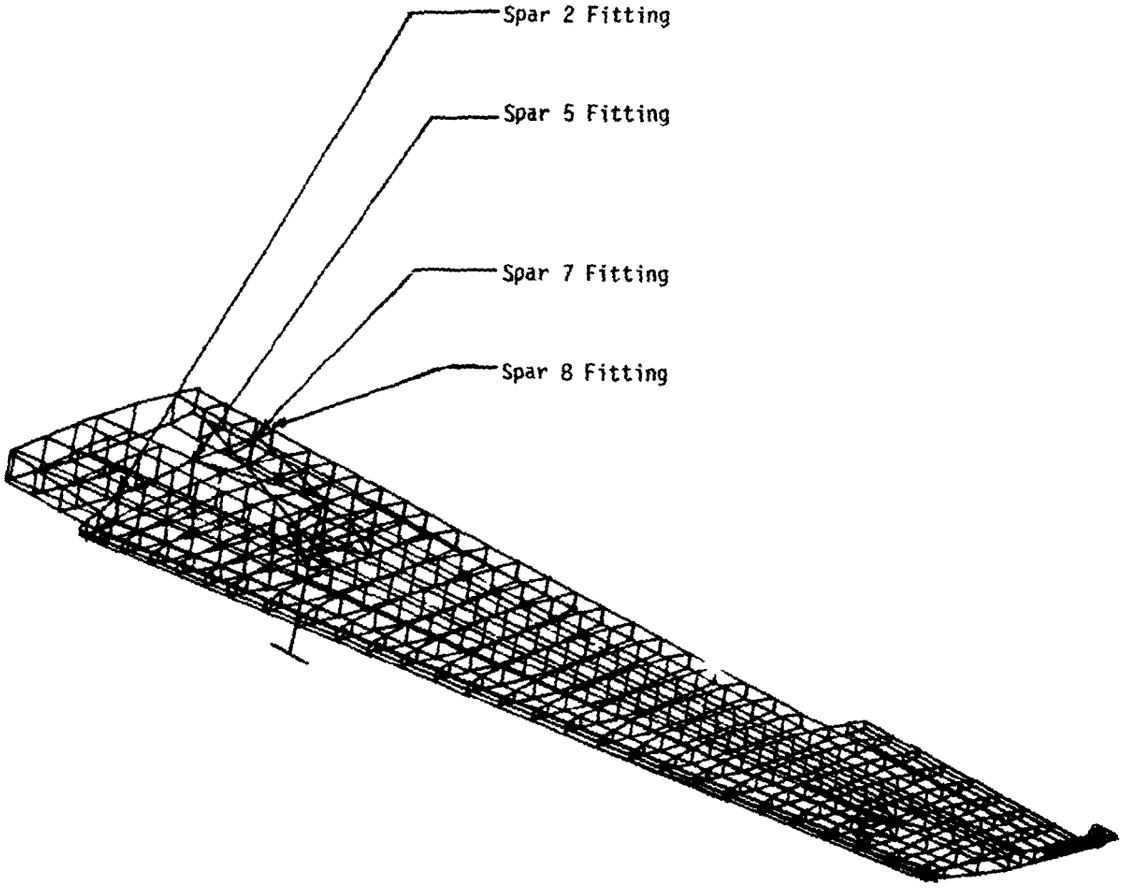

Figure 4 - Wing Attachment Fittings

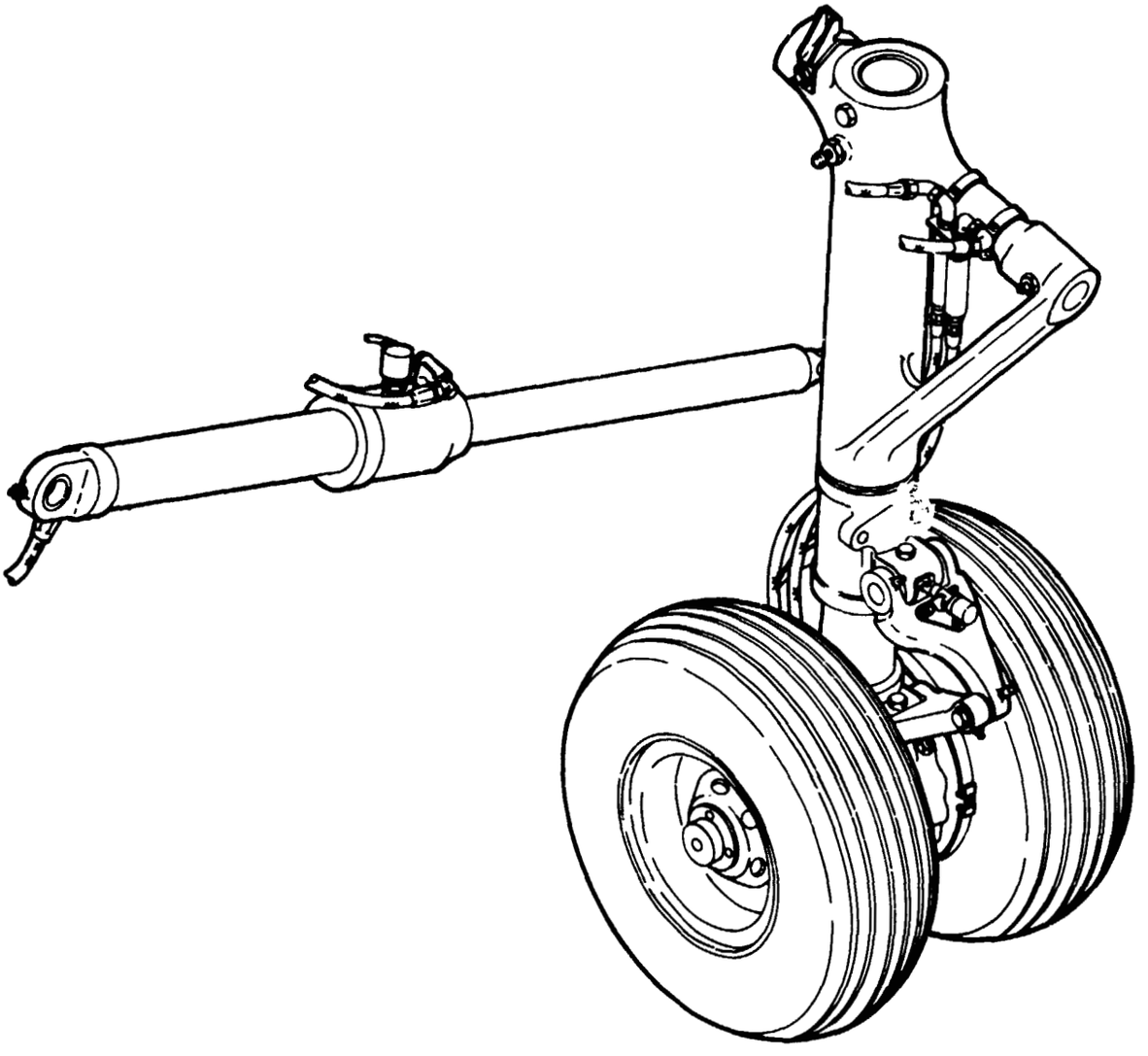

Figure 5 - Main Landing Gear

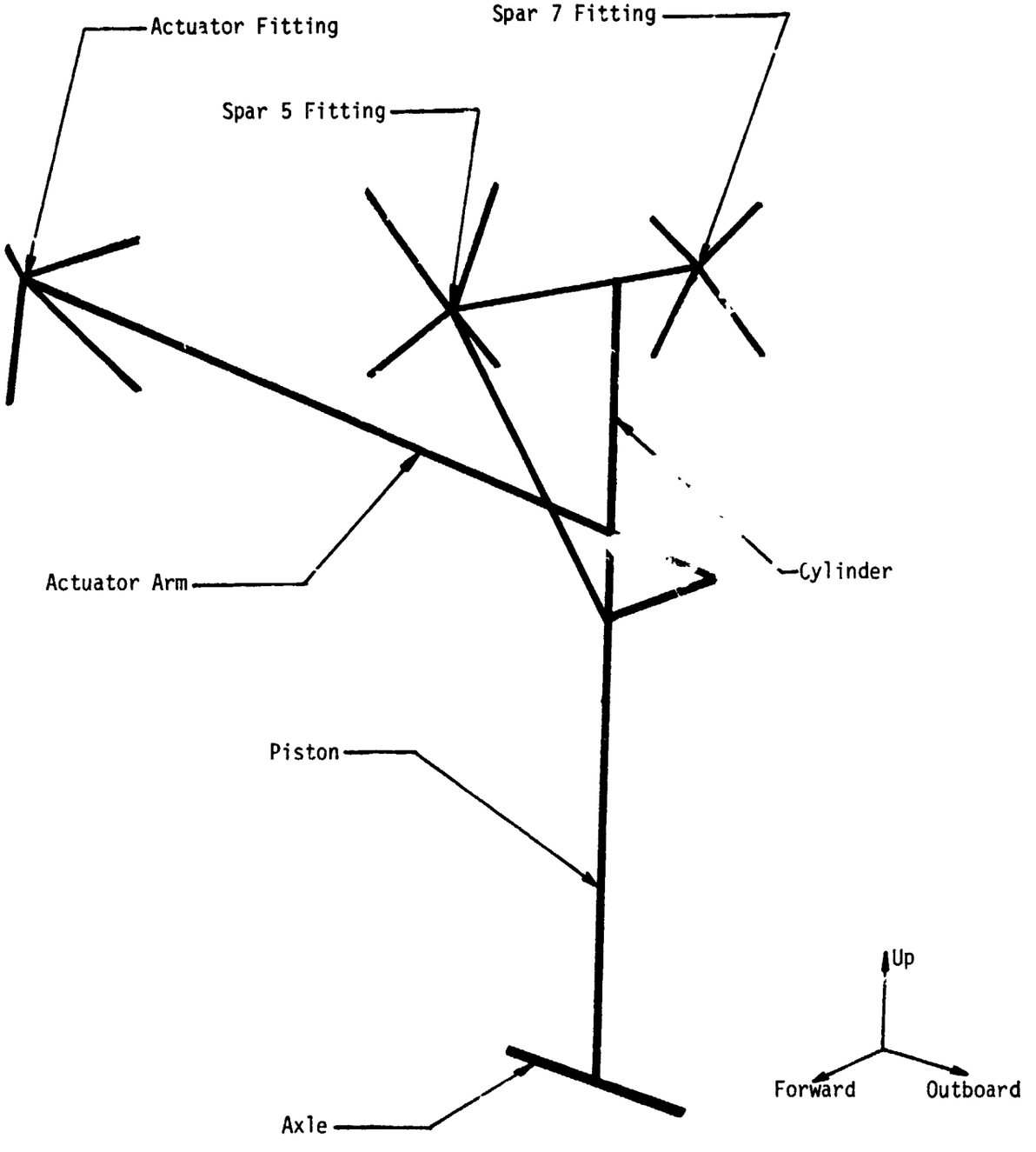

Figure 6 - Landing Gear Finite Element Model

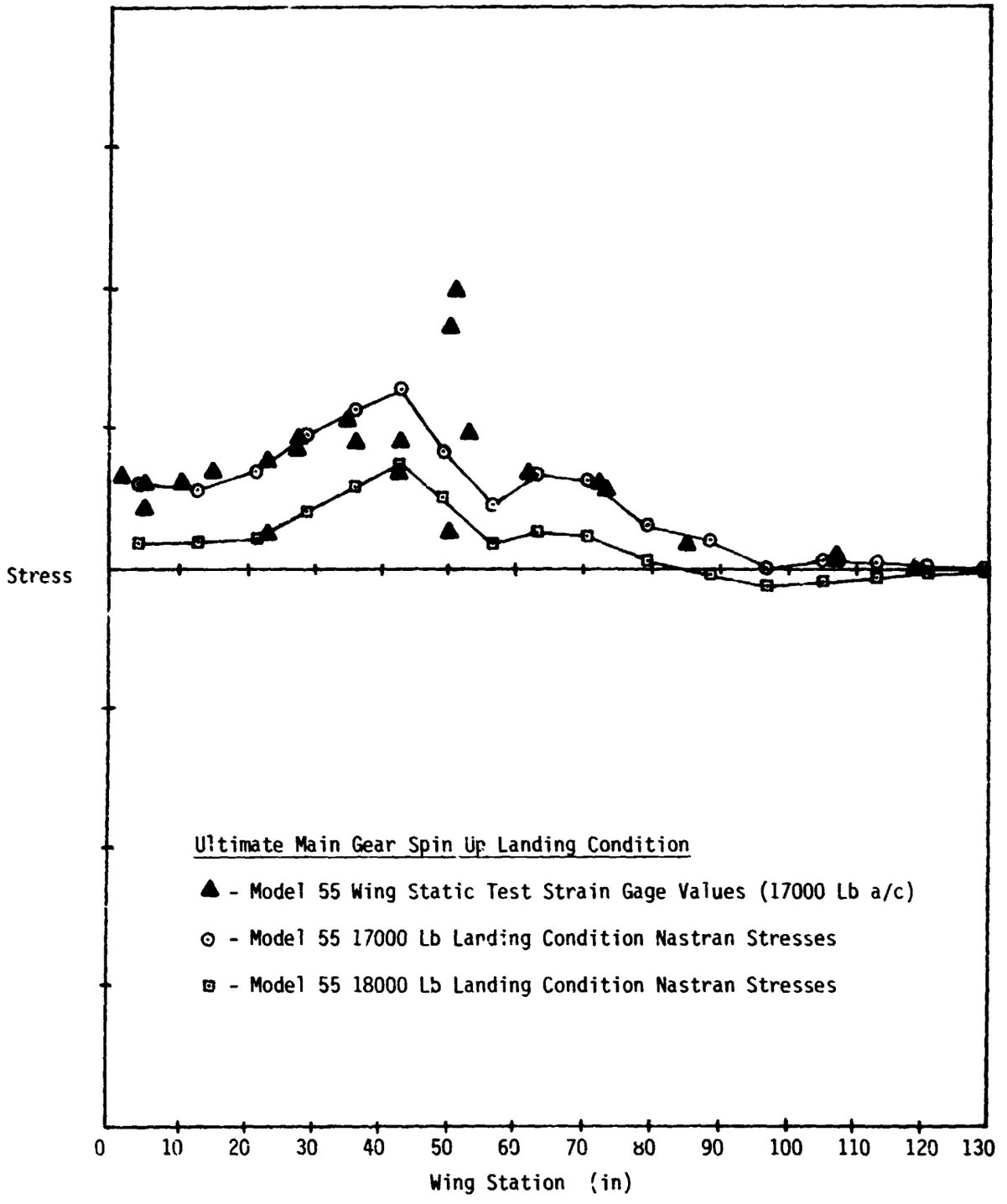

Figure 7 - Stresses In Spar 5 Lower Cap

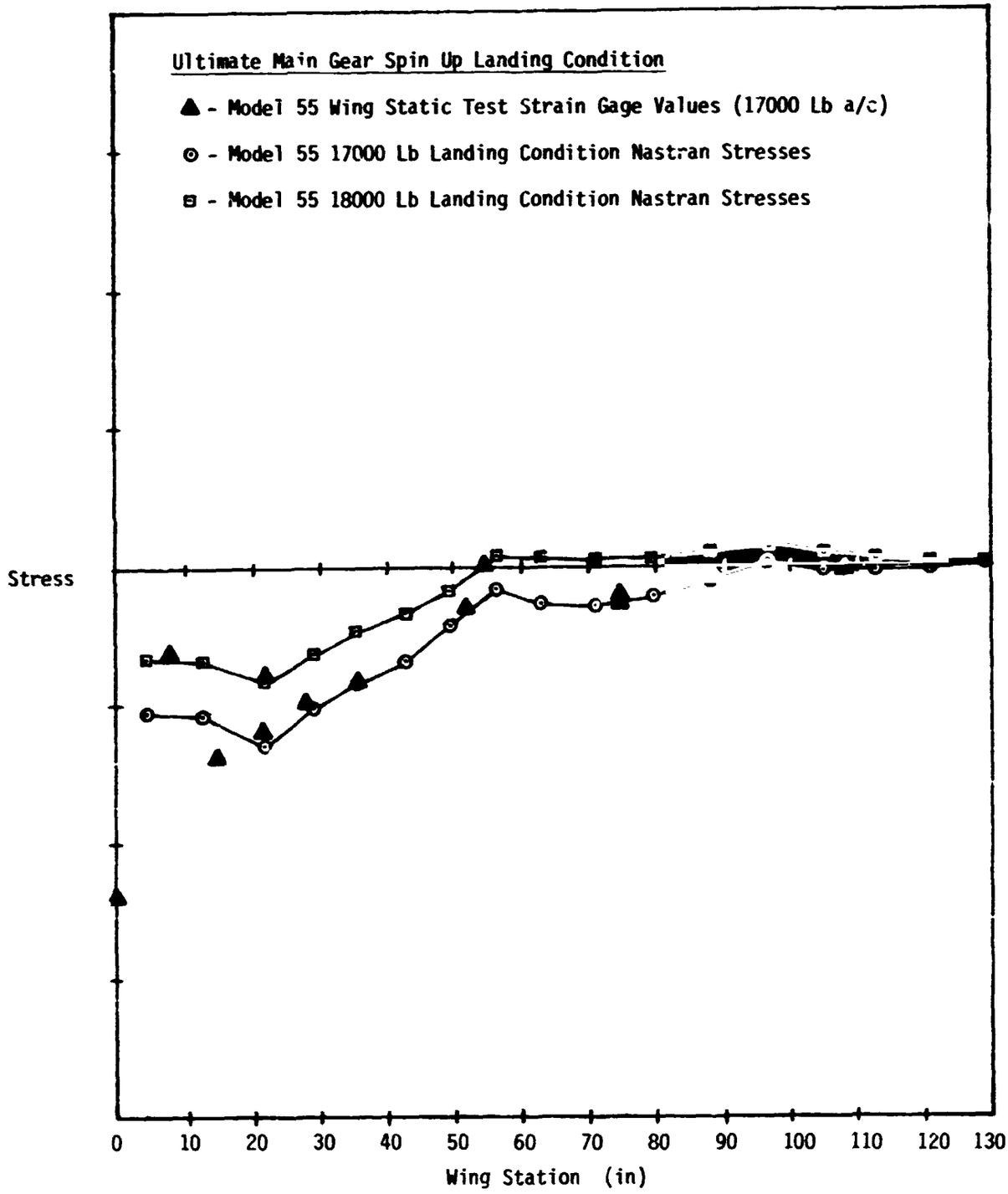

Figure 8 - Stresses In Spar 5 Upper Cap

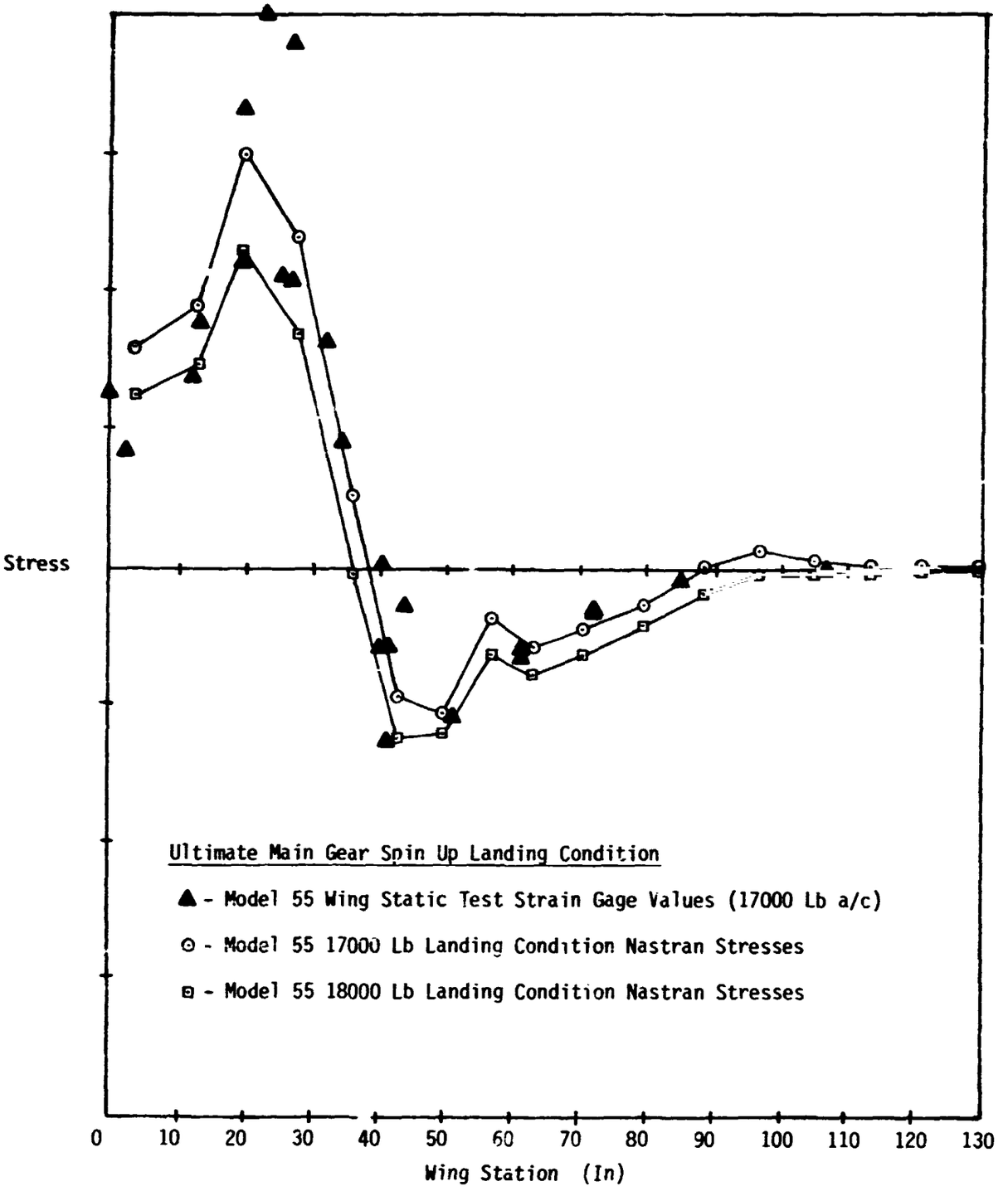

Figure 9 - Stresses In Spar 7 Lower Cap

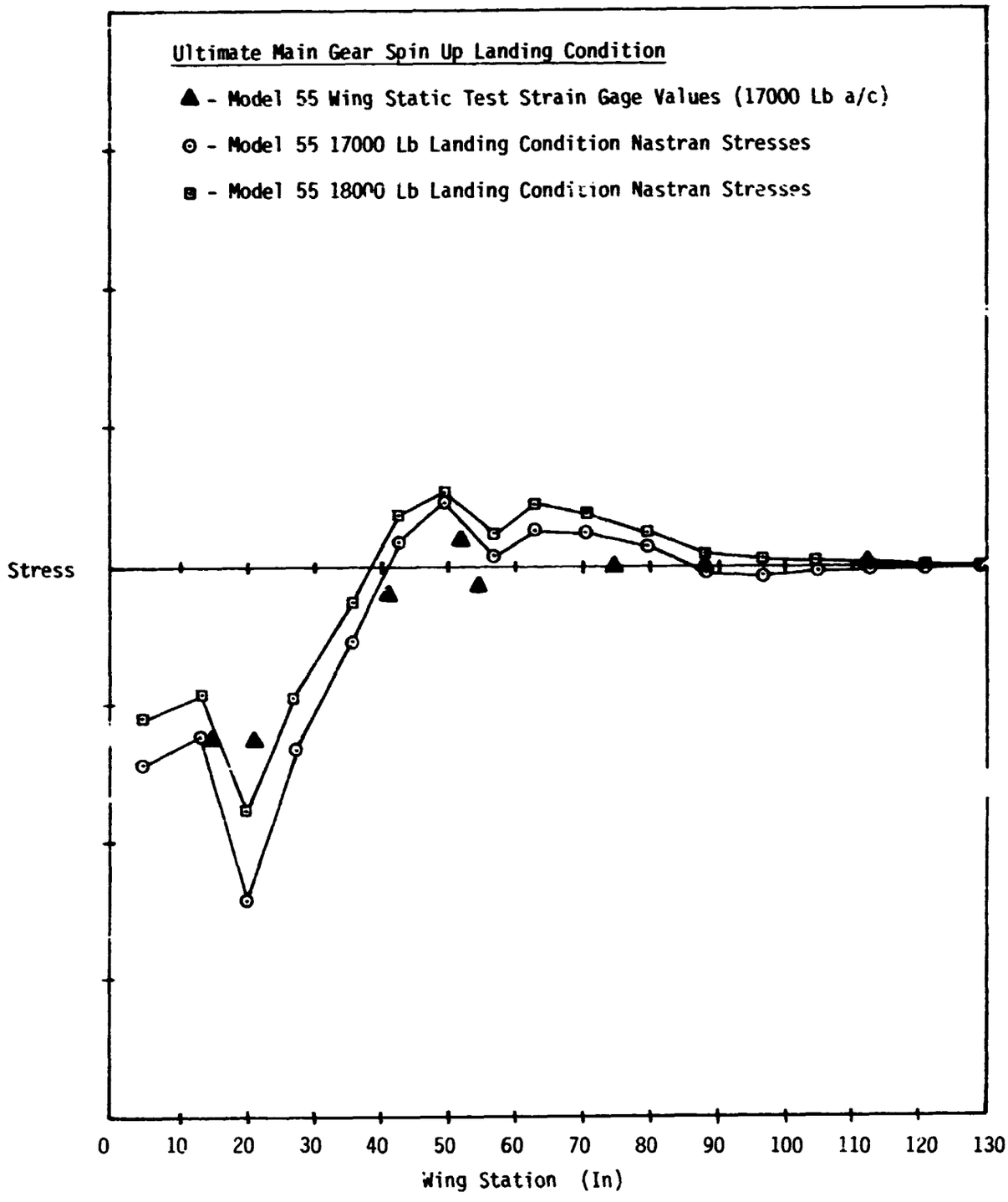

Figure 10 - Stresses In Spar 7 Upper Cap

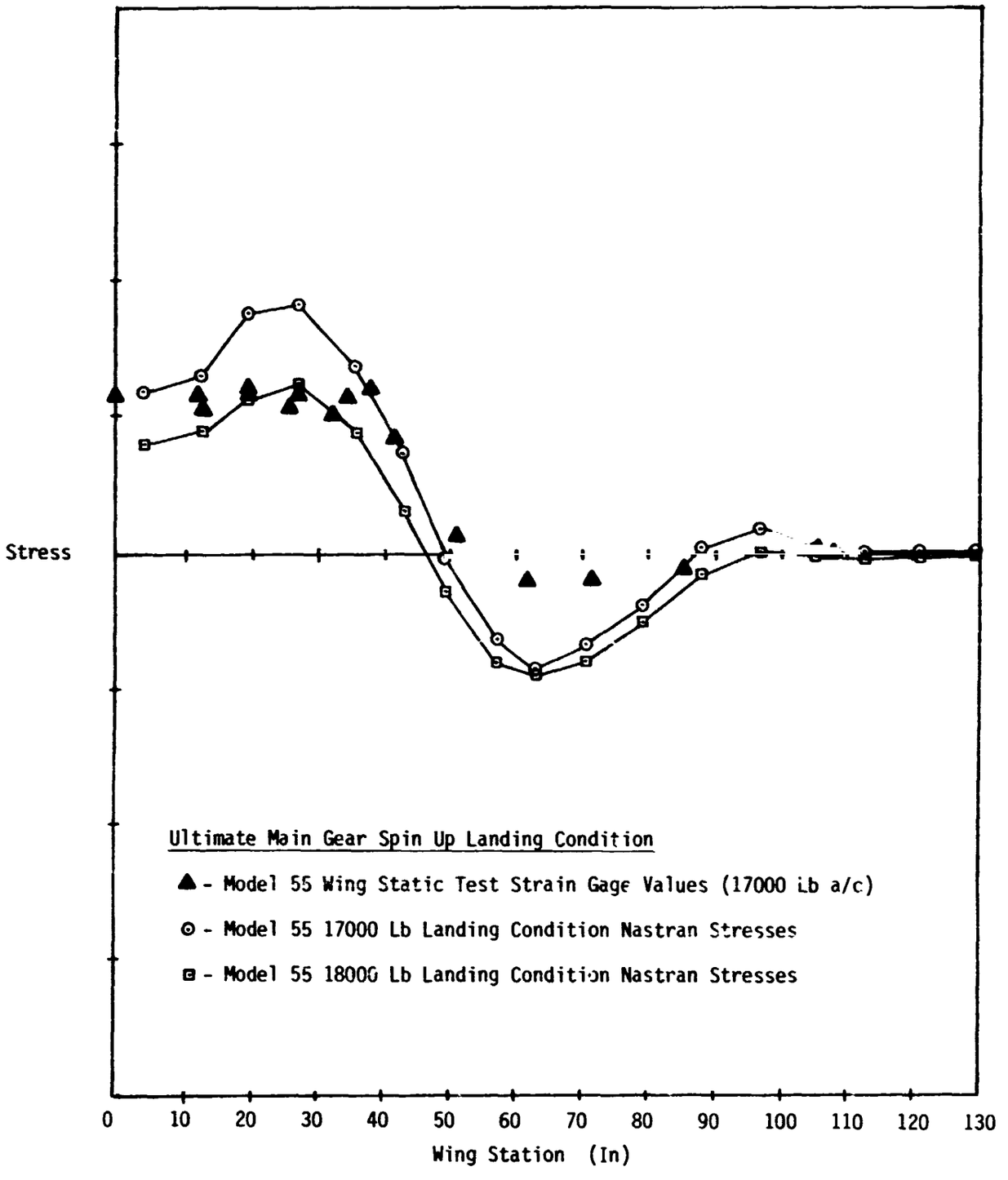

Figure 11 - Stresses In Spar 8 Lower Cap

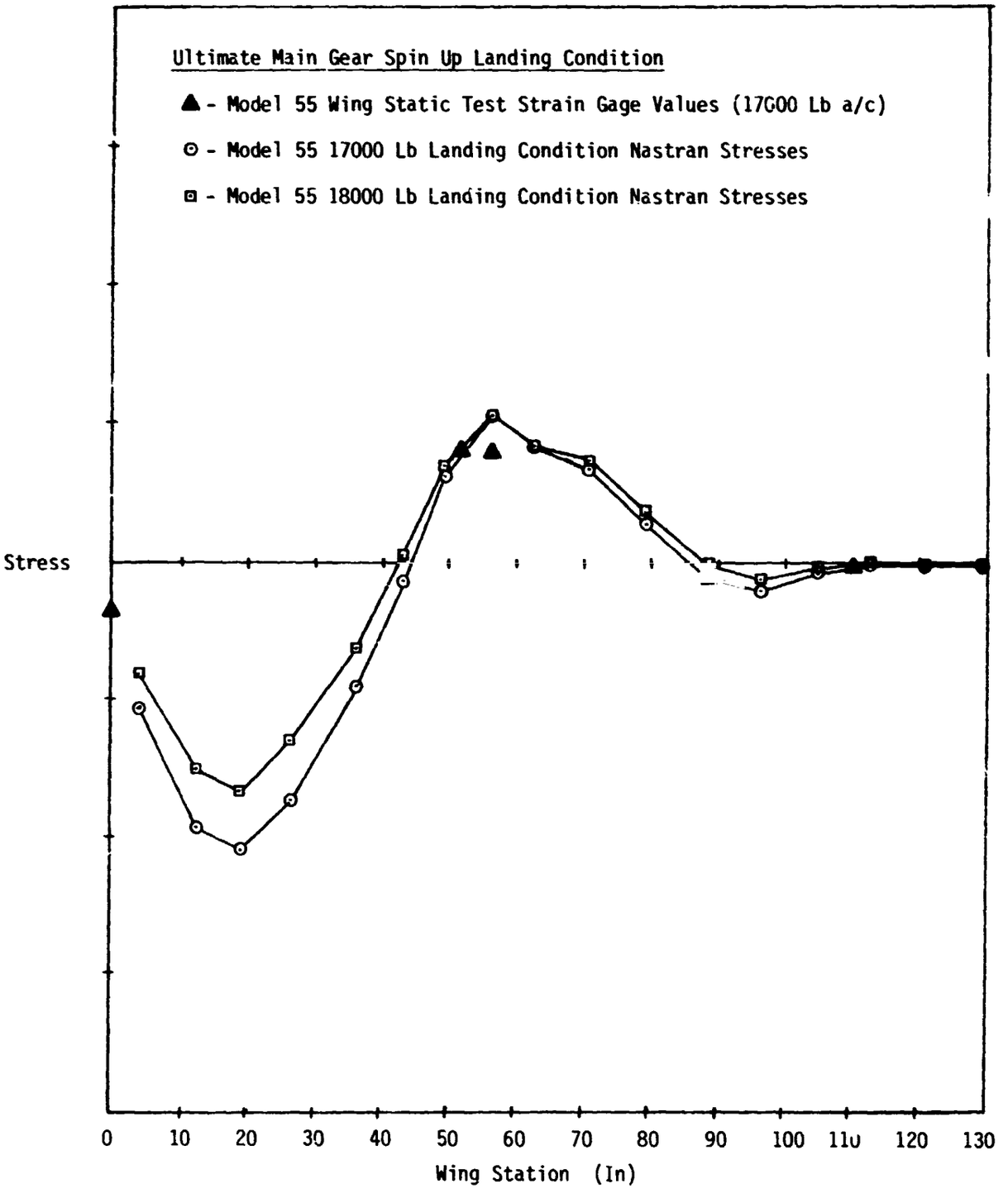

Figure 12 - Stresses In Spar 8 Upper Cap